

Customized shading solutions for complex building façades: the potential of an innovative cement-textile composite material through a performance-based generative design

Customized
shading
solutions

Received 19 January 2023
Revised 5 May 2023
Accepted 6 July 2023

Andrea Zani

*Department of Architecture, Built Environment and Construction Engineering,
Politecnico di Milano, Milan, Italy and Department of Architecture,
University of California, Berkeley, California, USA*

Alberto Speroni and Andrea Giovanni Mainini

*Department of Architecture, Built Environment and Construction Engineering,
Politecnico di Milano, Milan, Italy*

Michele Zinzi

*ENEA – Italian National Agency for New Technologies,
Energy and Sustainable Economic Development, Via Anguillarese, Roma, Italy*

Luisa Caldas

Department of Architecture, University of California, Berkeley, California, USA, and

Tiziana Poli

*Department of Architecture, Built Environment and Construction Engineering,
Politecnico di Milano, Milan, Italy*

Abstract

Purpose – The paper aims to investigate the comfort-related performances of an innovative solar shading solution based on a new composite patented material that consists of a cement-based matrix coupled with a stretchable three-dimensional textile. The paper's aim is, through a performance-based generative design approach,

© Andrea Zani, Alberto Speroni, Andrea Giovanni Mainini, Michele Zinzi, Luisa Caldas and Tiziana Poli. Published by Emerald Publishing Limited. This article is published under the Creative Commons Attribution (CC BY 4.0) licence. Anyone may reproduce, distribute, translate and create derivative works of this article (for both commercial and non-commercial purposes), subject to full attribution to the original publication and authors. The full terms of this licence maybe seen at <http://creativecommons.org/licenses/by/4.0/legalcode>

This work has been possible thanks to the experimental tests made with Jacobs institute UCB and Italcementi Group, and the support and assistance given by SEED Lab and UC Berkeley during the simulation process. This work, for the part related to material and methodology was also partially funded by “Ministero dello Sviluppo Economico (Mise)” through the grant Bando POC. The authors would like to thank also PA&CO that has provided facilities and equipment for the second phase of testing.



to develop a high-performance static shading system able to guarantee adequate daylight spaces, a connection with the outdoors and a glare-free environment in the view of a holistic and occupant-centric daylight assessment.

Design/methodology/approach – The paper describes the design and simulation process of a complex static shading system for digital manufacturing purposes. Initially, the optical material properties were characterized to calibrate radiance-based simulations. The developed models were then implemented in a multi-objective genetic optimization algorithm to improve the shading geometries, and their performance was assessed and compared with traditional external louvres and overhangs.

Findings – The system developed demonstrates, for a reference office space located in Milan (Italy), the potential of increasing useful daylight illuminance by 35% with a reduced glare of up to 70%–80% while providing better uniformity and connection with the outdoors as a result of a topological optimization of the shape and position of the openings.

Originality/value – The paper presents the innovative nature of a new composite material that, coupled with the proposed performance-based optimization process, enables the fabrication of optimized shading/cladding surfaces with complex geometries whose formability does not require ad hoc formworks, making the process fast and economic.

Keywords Form finding, Genetic algorithms, Innovative concrete component, Computational design, Digital fabrication, Shading device

Paper type Research paper

1. Introduction

Contemporary architecture is characterized by complex and aesthetically challenging shapes that push ahead the boundaries of traditional design approaches. Both for functional and aesthetic requirements, architects are motivated to experiment with new forms, as well as for the need to respond to social and environmental changing conditions. As new materials and construction technologies have emerged, the idea that “form follows function” has become a guiding principle in architecture. The traditional assumptions about form and structure needed to be reexamined, and new architectural paradigms explored.

The ability of parametric models to generate complex and customized outcomes can be limited by the constraints of the fabrication process (Oxman and Rosenberg, 2007); consequently, designers must compromise the ideal shape to accommodate production process limitations and to reduce manufacturing costs, resulting in a discretization of the geometries (Eigensatz *et al.*, 2010; Rörig *et al.*, 2015).

Given the increasing request for lightweight cladding and solar shading systems, several studies in the past few years have focused on the development of new cement-based materials.

Possible strategies include the use of different fibres (Banthia *et al.*, 2012) to be combined with the cement matrix in fibre-reinforced concrete (FRC), which uses both steel, glass and synthetic fibres, including carbon, nylon and polypropylene, to reduce cracking and control shrinkage phenomena under load.

Textile-reinforced concrete (TRC) is a type of cement-based material that uses noncorrosive textile fabrics as reinforcement. It is suitable for use in thin shells or folded structures, typically with thicknesses ranging from 10 to 20 mm (Valeri *et al.*, 2020). In addition, TRC can be combined with high-strength stainless steel bars to locally increase its load-carrying capacity in tension while maintaining low thicknesses and good workability.

Improved mechanical strengths and shorter setting time of concrete canvas can then be obtained by increasing anhydrite content or fineness in the cement (Han *et al.*, 2016). Extra performances, such as transparency, can be given to a generic concrete matrix through PMMA resin insertions in a FRC panel (Mainini *et al.*, 2012).

In architecture, an example of this new material trend is glass fibre-reinforced concrete (GFRC). Due to its workability and plasticity in the wet state, compared with its high robustness

when cured, it potentially represents a material for complex architectural shapes. However, the material potential clashes with the complexity and high costs of custom and unique moulds and jigs to meet the demand for complex shapes (Henriksen *et al.*, 2015; Henriksen, 2017).

In the standard production process, the formwork plays a crucial role in the construction of concrete structures, and it is the most significant cost in the overall realization process. Other than this, the selection of proper formwork systems and casting techniques depends on factors such as safety, structural geometry, construction time and surface quality (Li *et al.*, 2022). Improved processes include the use of algorithmic design, robotic fabrication and thermoforming methods to manufacture mass-customized elements with highly detailed and complex architectural components (Ruttico *et al.*, 2016).

An alternative to standard casting systems is represented by three-dimensional (3D) warp-knitted spacer fabrics introduced for use in concrete applications (Roya and Gries, 2007). These fabrics provide structures that are nearly net-shaped, load-adapted and handling-optimized. These fabrics can be impregnated by lamination, infiltration or concrete transfer moulding, especially fine-grained concrete matrices to make formworks or finite components. From an economic and production perspective, this is advantageous since it opens the door to new forming processes and makes the most of the formability of textile materials. An example of digital fabrication and computational design is 3D printing (Liu and Lv, 2022), which exploits the usage of synthetic polymer fibres and geopolymer mortars to 3D-print cement structures and components with increased flexural strength (Rael and San Fratello, 2011).

Using high-performance concretes allows printing large-scale complex geometries without the need for formworks while reducing the fabrication time and increasing both quality of the product and its mechanical resistance and thermal performance (Gosselin *et al.*, 2016).

Concrete materials have long been used for decades to make standard static shading systems, such as louvers and overhangs; however, it is a practice that the standard design process tends to separate the functions between exterior shading layers, high-performance glazing and interior shading devices, such as roller shades.

The separation of the function between the internal and external layers can be overcome by implementing a human-centric and generative design, as shown in the studies by Van Den Wymelenberg and Inanici (2014), Hashemloo *et al.* (2016) and Azadeh (2011). Both articles take into account each occupant's visual field of view while they carry out typical visual tasks in a certain environment, and the optimization path is then connected to a distributed sensing network of numerous occupants in the area.

Internal systems are provided to guarantee mainly visual comfort, and the research questions are related to material properties (Tzempelikos and Chan, 2016; Kuhn, 2017) and optimal shading control strategies (Tzempelikos and Shen, 2013; Katsifaraki *et al.*, 2017).

Manual shading controls lead to not well-lit spaces because of the lack of interaction between users and shading systems (Van Den Wymelenberg, 2012; Sadeghi *et al.*, 2016). Hence, a well-designed static shading system can overcome this limitation, providing better performance on an annual basis.

Several consolidated approaches to design an optimal static external shading system already exist: the identification of the cut-off date and time; the use of overshadowing dynamic patterns (Arumi-Noe, 1996; Kabre, 1998); the use of shading masks considering different sky-subdivision techniques (Marsh, 2005) or thermal and daylight metrics optimization (Sargent *et al.*, 2011). Going more into detail, the generative performance-based design approaches allow studying complex perforated shading surfaces, aiming at controlling sunlight while improving daylight and/or reducing the occurrence of glare. One first significant example can be found in the optimization of a Mashrabiya pattern through the arrangement of its non-uniform perforation ratio (Sherif *et al.*, 2012). Detailed innovative

approaches involve the use of bidirectional light transmission methods to compute scattering and interreflections through a shading screen and for the assessment of the daylight distribution in a room (Omidfar, 2015).

The use of a genetic algorithm (GA) based method was already positively tested in generating and optimizing the geometry of an innovative concrete shading system able to both improve thermal and visual comfort (Zani *et al.*, 2017). The creation of static geometry shading systems through generative techniques can lead to the development of intricate designs, and the vast size of the space of solutions presents a significant challenge for evaluating a large number of possible alternatives. Manual evaluation is impractical due to time constraints. One potential solution is to use stochastic techniques, such as evolutionary algorithms. These algorithms operate on a cyclical basis, searching through generations of design solutions (populations) using operations like recombination, mutation and selection to progressively shift successive generations towards solutions that perform better when evaluated based on a specific criterion or multiple criteria (fitness function) (Turrin *et al.*, 2011, 2012). These methods were tested in exploring the morphology of a roofing semitransparent surface, considering the structural performance, such as the solar energy transmission, solar heat gain coefficient and daylight. Other relevant studies about daylight optimization used different tools such as Matlab (Rakha and Nassar, 2011), GeneArch (Caldas and Norford, 2003a, 2003b) or Grasshopper-based evolutionary solvers, such as Galapagos or Octopus (Zani *et al.*, 2017; Madkour, 2023; González and Fiorito, 2015) to develop a performance-based generative design approach.

This research aims to demonstrate that it is possible to combine a novel, performance-driven generative design approach with an innovative cement-based material to create an external shading system that effectively controls thermal and visual performance while also optimizing the production process. Hence, the possibility the cement textile component could bridge the gap between free-form geometry design and fabrication is discussed. In addition, digital fabrication enables the reevaluation of fixed systems, making them once again become a viable design alternative for solar shading through the ability to modify not only the shape but the openness factor, the pattern and the texture while answering performance requirements.

To achieve this result, experiments and preliminary simulations were conducted to comprehend the innovative concrete's optical characteristics. In the second part of the study, an occupant-centred generative design methodology was developed for an external shading system, reducing the need for an additional internal shading layer. Finally, a case study model created using a parametric and GA methodology was compared with the performances of conventional concrete shading systems, such as overhangs and louvres.

2. Cement-textile composite

Nowadays, the most used materials for the production of thin cement-based customized elements, such as façade panels and solar shading, are GFRC and ultra-high-performance concrete. The free-form facade demand has led to an increment in manufacturing costs of the facade because of the complexity of mould systems necessary for the production process and the high number of unique moulds. Furthermore, these moulds have to be considered and analysed also for their impact in terms of global warming potential (GWP) being mainly a single-use disposable element.

Within the defined context, cement-textile composite (CTC) aims to simplify the manufacturing process by making formwork not necessary. Indeed, this is possible because of the intrinsic properties of the process that works by using non-returnable frames and local tension and/or compression forces applied. This makes it no longer necessary to have moulds.

The new composite material is produced with an innovative manufacturing technique that consists of a 3D-warped knitted polyester fabric combined with a tailor-made cement mix (POLI *et al.*, 2019). Figure 1 presents a schematic comparison between the standard fabrication process of a complex building surface and the CTC production processes. By comparing the two, it is possible to identify that CTC better optimizes the production phase by avoiding the moulds [Figure 1(N.3)] need and consequently – as previously described – reducing scrap material [Figure 1(N.7A) and (N.7B)], costs and consequently GWP impact.

The thickness of the material varies between 3 mm and 12 mm, and the total weight is between 5 and 15 kg/m². The elasticity of the knitted fabric allows to manufacture of elements with different shapes (from planar to double curvature) and dimensions without the need for formworks, but relying only on frames and localized tensile and compression loads. It can be customized with infinite surface texture, and it allows control of the translucency of the panel by removing part of the cement mix, as described in Poli *et al.* (2019).

The spacer fabric can have different features: Textile 1 (Figure 2) is a 7 mm spacer with the same stretchable back and a front surface texture separated by a consistent interlayer

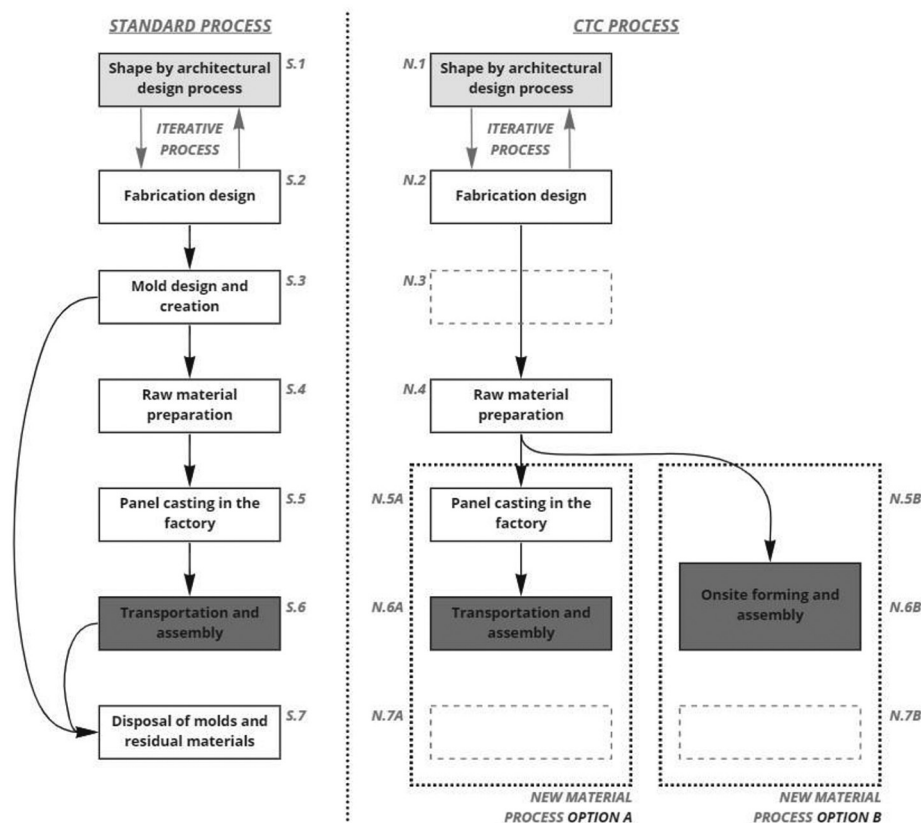


Figure 1.
Comparison between
the standard
fabrication process
and CTC process

Source: Created by author

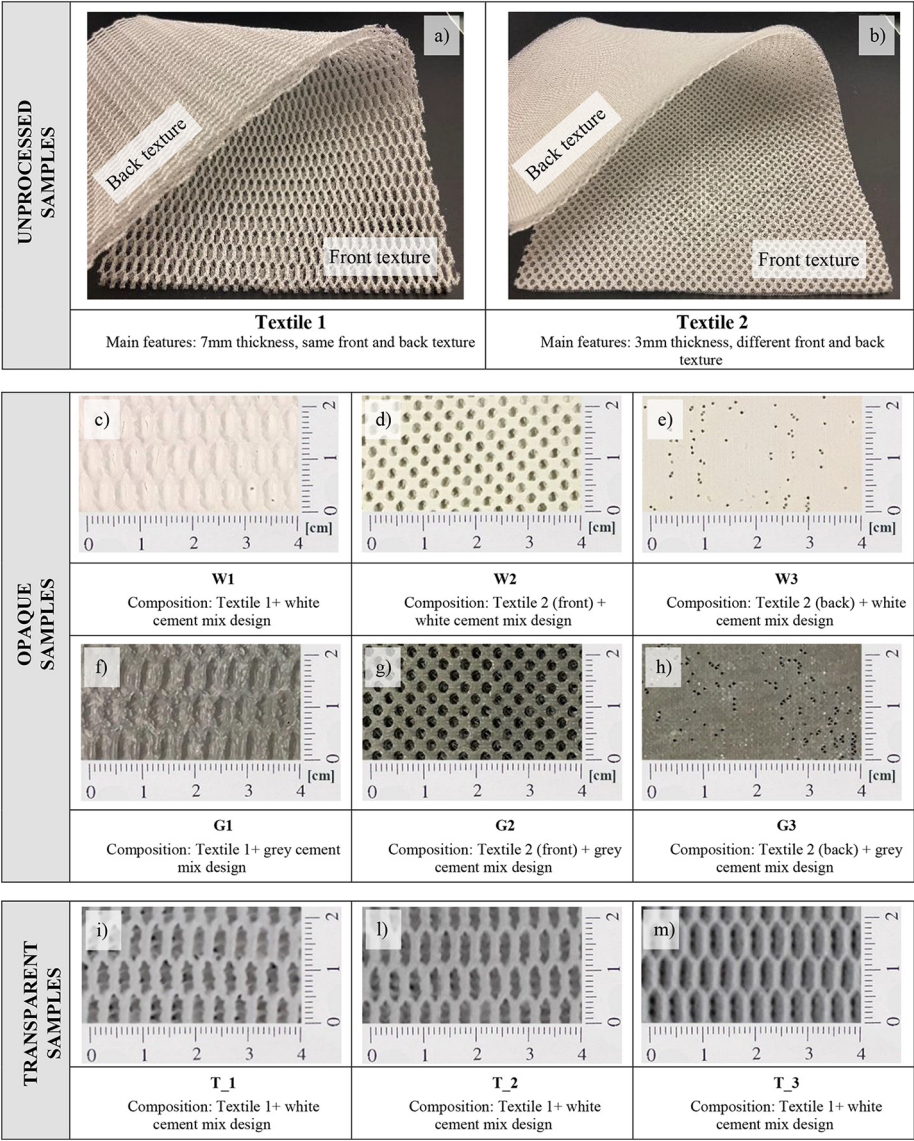


Figure 2.
CTC possible
material
configurations

Notes: Unprocessed samples (textile 1(a); textile 2(b)); opaque samples (W1(c), W2 (d); W3(e); G1(f); G2 (g); G3(h)); and transparent samples (T_1 (i), T_2 (l), T_3 (m))

able to maintain the two layers at the same distance while Textile 2 (Figure 2) is a 3mm spacer with low permeability stretchable back and a wider texture front surface separated by a consistent interlayer. In both of the two selected 3D spacer types, the front textile surface has to be permeable to allow the fluid-bonding compound to pass through; it can be

weaved with any texture based on the desired pattern, elasticity and openness factor requirements. The back layer of the spacer may have lower permeability to prevent the semi-liquid mix to run through. The cement matrix rheological behaviour has been customized to have specific fluidity and homogeneity according to the fabric characteristics, such as the openness factor of the front surface and the space between interlayer yarns. Fluidity and filler dimensions can be easily changed in function of the different possible configurations, and at the same time, they have to guarantee enough workability, good stiffness and rigidity.

Moreover, the selection of a 3D fabric is crucial in achieving the target shape. If the fabric's elasticity is inadequate, it may be necessary to implement joining lines, which are determined through the optimization process outlined in Figure 3 as part of the “production design optimization process”. However, a detailed analysis of this process is beyond the scope of this paper and will be presented in future works.

Figure 3 presents an overview of the entire process. The diagram refers to a target shape alternative (which corresponds to the optimized standard-based solution presented in the following daylighting analysis. However, it is possible, through the developed process (Poli *et al.*, 2019), to obtain multiple complex geometries through localized/diffuse tensile and compressive actions/stresses, which exploit the elasticity and directionality of the fabric. The workflow can be divided into three phases: design, in-plant production and onsite operations. The design phase consists of three consequential iterative stages that are: the architectural design process, daylighting optimization process and the production optimization process. A more detailed description of these processes is presented in Figure 4 as a core topic of the paper. The in-plant production phase consists of the preparation and preassembly of the three main components (frame, fabric and concrete) whose features arise from the outcome of the optimization process carried out. In the onsite phase, on the other hand, it is planned that the components are assembled, the fabric is installed through tension/compression actions and the previously defined cement mixture is then applied.

Figure 2 shows three different samples per colour (white and grey) of opaque CTC. Three different textures have been selected to understand their influence on spectral and overall

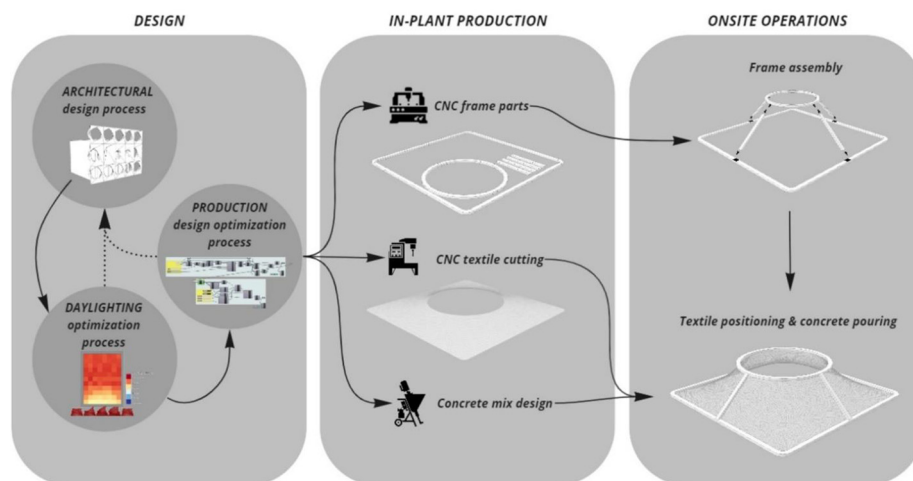


Figure 3.
CTC workflow:
design phase, in-plant
production and onsite
operations

Source: Created by author

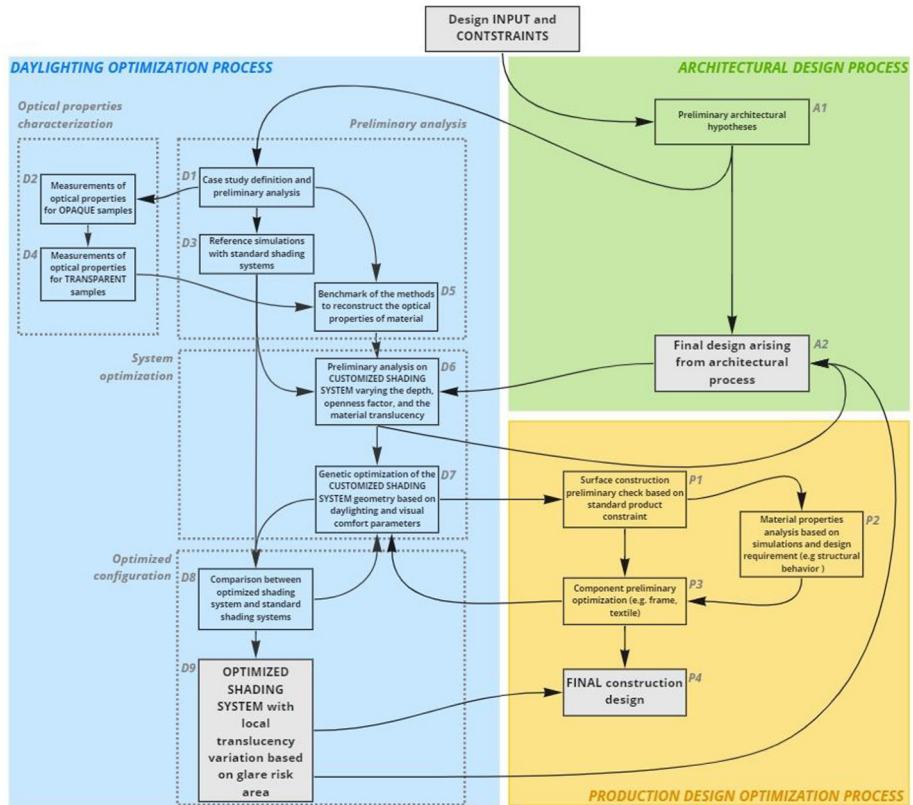


Figure 4.
Detailed description
of the design process
(as per the general
workflow from
Figure 2)

Source: Created by author

reflectance values. Samples (c) and (f) are composites solutions with the same 3D textile but different cementitious (white and grey) matrices featured by the same texture for the front and back that has rhomboidal holes texture with a height equal to 8 mm and width of 4 mm. Samples (d) and (g) are composites solutions with same 3D textile featured by a denser pattern with holes diameter equal to 1.5 mm. Samples (e) and (h) instead are the back side of, respectively. Samples (b) and (e) have a continuous opaque surface without any visible texture. Samples (c), (d) and (e) are made with the same white cement (with different mix designs), while samples (f), (g) and (h) are made with the same grey cement (with different mix designs).

One of the most outstanding features of CTC, in comparison with the traditional cement-based material, is the possibility to have translucent components. Adjusting the amount and the distribution of cement mix or removing it locally, it is possible to control the translucency of the element, creating specific light patterns. The translucency of the panel can also change based on the texture of the 3D-warp textile. The hybrid feature of the CTC that blends fabric characteristics, such as texture, translucency and ductility, and thin-shell tectonics represents a potential cutting-edge technology for the development of free-form building envelope components such as high-performance solar shading systems.

3. Methods

The objective of this study is to quantify the technical potential of a novel cement-based material coupled with a performance-driven generative design approach applied to a shading system to reduce energy use while improving visual comfort. Indeed, this feasibility owes to the flexibility in the process of shape manufacturing, enabling the fulfilment of geometric and architectural requirements while maintaining cost-effectiveness. The daylight-driven optimization design workflow (Figure 4) starts from the architectural requirement [Figure 4(a), green area identified by “Architectural design process”] and follows by involving two process tools/workflows created for the purpose. The first relates to the performance parametrization [Figure 4(a), blue area identified by “Daylighting optimization process”] required for the target surface, and the second relates to the feasibility and optimization of production [Figure 4(a), orange area identified by “Production design optimization process”] with a view to digital fabrication. In this paper, only the first of the two tools was tested, and the method and main results of the process will be presented. The evaluation of the energy and daylighting performance of complex shading systems was performed mainly through computer simulation after a series of experimental measurements to assess the material properties and calibrate the material definition in the simulation environments.

The methodology developed for the present study consists of the following phases:

- Measurements of the optical properties of several options of the new material, both opaque and transparent [Figure 4 (D2) and (D4)];
- Choice of the methods to benchmark [Figure 4 (D5)] the optical properties of the material (radiance translucent material definition compared with the bidirectional scattering distribution function [BSDF]);
- Preliminary analysis of the shading layer shape varying the depth, openness factor and the material translucency/opacity [Figure 4 (D6)];
- Genetic optimization of the shading geometry based on daylighting and visual comfort parameters [Figure 4 (D7)];
- Optimized local translucency/openness factor variation based on a glare risk area method; and
- Comparison between optimized shading system and standard concrete shading systems [Figure 4 (D8)].

3.1 Measurements: optical properties

To assess the daylight performance of the CTC-based shading system, the main optical properties useful for the material characterization have been measured. Given the discontinuous nature of the material cement and the random filling pattern provided, nine different configurations have been tested with different textile textures, colours and translucency.

The optical characterization, including solar transmittance, reflectance and absorbance, was performed using two instruments: a spectrophotometer LAMBDATM 950 and a large integrating sphere facility (Maccari *et al.*, 1998).

The spectrophotometer used for these measurements of the entire solar spectrum (250–2,500 nm) was located at the SeedLab Facility at Politecnico di Milano, equipped with a 15 cm integrating sphere coated in white Spectralon® film. Because of the light beam dimension (1.2×0.7 cm), the instrument was suitable for analysing opaque materials or

materials with a dense continuous texture. Among this latest option, 3D textiles filled with the cementitious matrix can be included. The selected translucent sample, characterized by a large texture that could not have been fully sampled by the measuring beam of a standard spectrophotometer, was measured by a large integrating testing sphere facility. This procedure avoided a significant deviation of the measured results depending on the positioning of the sample, over the measuring port and under the light beam. The large integrating sphere (75 cm in diameter) used is equipped with a light source representative of the first part of the solar spectrum (300–1,750 nm) and a diameter of 7 cm, with a goniometer serving as a lamp support for angular measurements.

To understand their light transmission, three samples with different transparency have been prepared and measured with a modified integrating sphere. T_1 sample [Figure 2 (i)] has the lowest light transmission value, and the sample T_3 [Figure 2 (m)] has the highest translucency that can be obtained using this typology of 3D spacer fabric.

Each sample has been measured in three different positions, over the front surface, to take into account the influence of the fabric texture. The measurement spots were randomly chosen over the surface of the sample just to be representative of a minimum standard deviation of the possible expected measurement result. Then the average spectral curve and the average broadband values were computed according to ISO 9050 for transmittance reflectance and ASTM E903 for reflectance.

3.2 Models, materials and shading device configurations

The proposed simulation workflow is applied to a conventional Italian single office located in Milan (45° 28' N, 9° 10' E), in the northern part of Italy, facing south and west. The dimensions of the single office are 3 x 4 x 3 m (W x L x H), and it is side lit from a curtain wall system with a window-to-wall ratio (WWR) equal to 87% and a glazing unit having 0.7 of visual transmittance. The internal surfaces adjacent to other offices are adiabatic and with typical reflectance values according to Brembilla et al. (2017) and CIBSE AM11, except for shading materials stated in Figure 5. Experimental results and preliminary calibration analyses are presented, respectively, in Sections 4.1 and 4.2.

To fully exploit the construction possibilities offered by the new material, it was decided to foresee a funnel geometry that could represent one of the minimum surface deformations

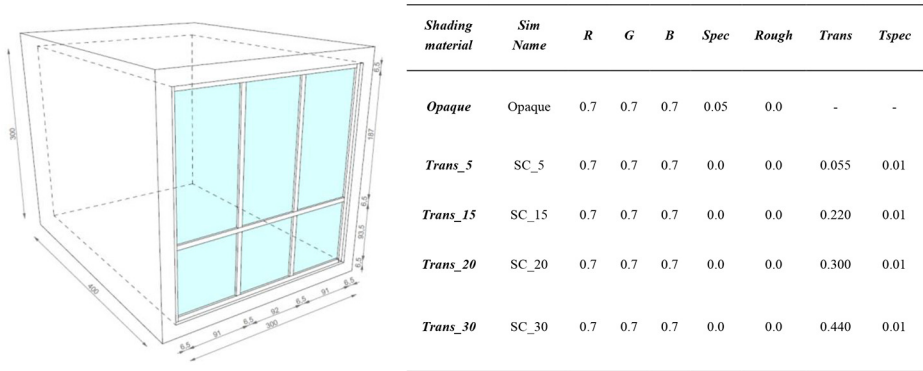


Figure 5. Single office case study – shading system material radiance definition

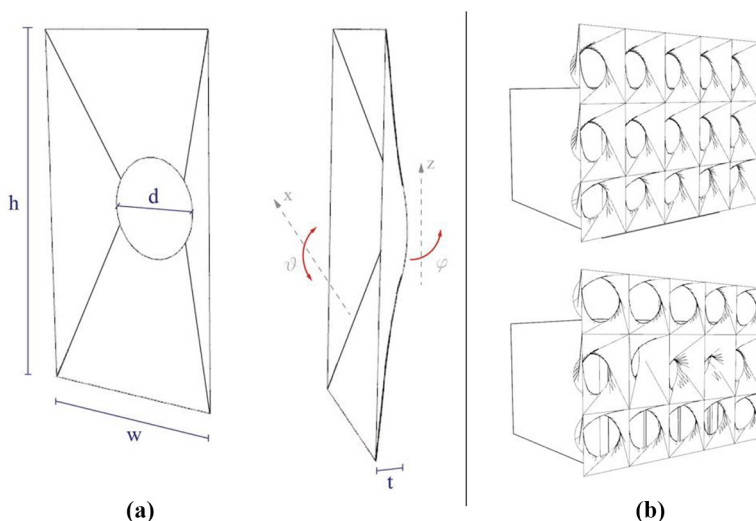
Source: Created by author

of a planar elastic fabric. The authors are aware that funnel geometries are not commonly used in facade applications in contemporary architecture, however:

- The authors wanted to steer away from standard planar geometries mostly used in current practice and explore the performance potential of complex double curvature taking advantage of the elasticity/deformability of the proposed material. This is only one of the possible combinations and possibilities that can be implemented, as described in the patent (Poli *et al.*, 2019);
- The process of modifying the geometry, although entrusted to a few optimization parameters, determines substantial changes in the final shape and allows to regulate the amount of direct and diffuse sunlight passing through the system;
- Based on the user's view and light source direction, the ratio between the dimension of the opening and the depth of the funnel is then defined, such as the ratio between the opaque and transparent portion of the surface.

The funnel, represented in Figure 6, is characterized by a rectangular base and circular opening. The base dimensions can vary according to facade module dimensions and facade aesthetics pattern, with maximum dimensions driven by the mechanical resistance of the CTC and the loads acting on it.

In this proposed optimization, the opening diameter can vary from a minimum of 10 cm to the width of the panel minus the 10 cm edge zone. Varying the opening dimension [d in Figure 6(4)] is possible to modify the panel openness factor from 5% to 40%–50%. Other possible geometrical variables in the funnel component are the depth [t in Figure 6(4)] and



Notes: (a) Funnel variables considered in the simulations; (b) examples of Funnel shading applied to the case study

Source: Created by author

Figure 6.
(a) Fabric Concrete funnel variables: panel height (h), panel width (w), diameter (d), shading depth (t), hole rotation (ϕ) and hole tilt (θ). (b) Two examples of funnel shading system. the images are indicative; they are not representative of the model, where the panelling used was such as to cover the entire transparent surface of the façade. Continuity was ensured by overlapping more than two rows of panels to avoid the radiation bypassing the shading system

the XZ position of the opening. Furthermore, due to the high flexibility of the material is possible to rotate in two directions (θ and ϕ) the plane of the openings with a variation up to $\pm 30^{\circ}$ – 40° in both directions. All the parameters can be optimized based on the desired occupant-centric performance goals. Please note that the possible geometrical extents of the panel are related to the elasticity of the textile used for the component, such as the way in which the material is tensioned and framed. Particular shapes may require a discontinuous geometry realized by stitching the fabric.

In the case study, the façade height has been divided into two modules with a dimension equal to 1×1.4 m (in Figure 6, respectively, w and h). Hence, it is possible to have better control of the geometry, to guarantee high flexibility in terms of openness factor and to reduce the risk of underlit space and lack of light uniformity. Elements with repetitive geometry can be implemented, however, and to fully benefit from the capacity of CTC, customized elements have been developed and analysed, as shown in Figure 6 – bottom right, where every panel presents a different geometry.

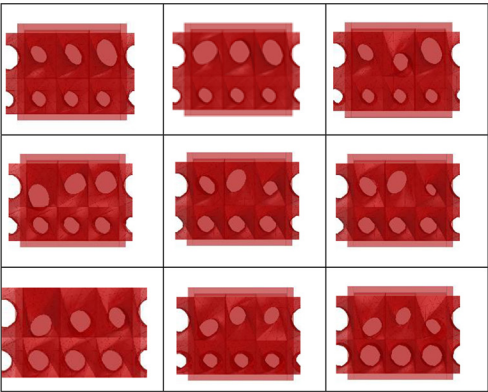
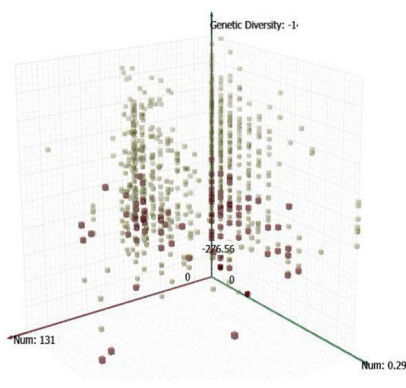
In the first set of simulations, all the funnel elements present the same material definition with average translucency, based on Figure 7. In the final set of simulations, based on a similar approach presented by Hashemloo *et al.* (2016), the performance of the funnel shape was assessed with the translucency gradient based on the glare risk distribution on the façade plane.

The façade area affected by potential glare will be masked by the self-shading effect created by the shading geometry. Instead, the other parts of the façade with limited glare risk will provide a connection with the outdoor, adequate illuminance level and the right balance between winter and summer solar gains. Combining these features with the control of the translucency, a smooth transition can be obtained between the opening and the shading element, avoiding high contrast between the two areas.

3.3 Simulation and optimization process

This paragraph presents the simulation methodology and settings used to assess the daylight and visual comfort performance of the solar shading configurations presented in the previous section. Four daylight metrics were used to evaluate work-plane illuminance and daylight distribution as daylight autonomy (DA), spatial daylight autonomy (sDA),

Figure 7. Visual representation of genetic algorithm outputs: dots in the diagram represent possible optimized solutions and red façade are some of the possible representation



Source: Created by author

useful daylight illuminance (UDI) (Carlucci *et al.*, 2015) and spatial useful daylight illuminance (sUDI). Simultaneously, point-in-time and annual glare analysis using the daylight glare probability metric (DGP) (Wienold, 2009) were carried out to estimate the number of hours and the intensity of possible glare discomfort. The parameters were chosen to guarantee high accuracy and stability of the results and, at the same time, to limit the calculation time. The machine time, especially for complex geometries characterized by dense mesh distribution, can rise exponentially. All the analyses were done in a Rhino-Grasshopper-based environment, using Radiance in Ladybug tool.

Given the atypical optical behaviour of the proposed material, preliminary simulations were necessary to implement the most suitable Radiance material definition. In particular, two different definitions of translucent (Trans) materials have been tested. The first is based on Mead (2012), and the second is according to the Radiance standard set-up (Reinhart and Andersen, 2006). The main difference between them is the value of the RGB channel. The first definition changes the RGB values following the other four parameters that define a translucent material. Instead, in the second characterization, the RGB values are set as input based on the measured visible reflectance of the materials.

The choice of the material definition was considered adequate due to the simplicity of the resulting calculation model, resulting suitable for iterative optimizations and the mainly scattering nature of the measured translucent samples. Alternative reconstructions, such as the definition of a BSDF for the material, would have required reconstruction of the geometry of the fabric. This could have been done by parameterizing the spatial and 3D distribution of the thread, considering an eventually increased thickness due to concrete deposition, such as a random filling pattern, considered as an attempt to reconstruct, even partially, the on average crossing section of the sample. The latter approach was considered too aleatory and prone to possible errors that could not be checked or repeated. For this reason, it was preferred to limit the translucency of the material to a small percentage (15%) and to entrust its description to a standardized methodology (Mead, 2012; Reinhart and Andersen, 2006). Starting from the results obtained in the preliminary calibration simulations, the material definition has been specified to better approximate the CTC optical behaviour, while the minimum openness factor range necessary to guarantee proper DA was found to be greater than 50%. These properties were applied to the complex funnel geometry described in Section 3.2 with the intent to improve the overall system performance.

Before running the optimization algorithm, a parametric sensitivity analysis was conducted on the funnel shape to understand the influence of each geometric parameter on the overall daylight performance and minimize the number of variables/combinations controlled by the GA. In particular, one opaque material, two translucent materials (SC_15 and SC_20), two openness factors (20% and 40%) and five different funnel depths (0, 10, 20, 30 and 50 cm) were analysed. These alternatives serve to indicate a panorama of hypothetical acceptable solutions to meet performance requirements. They will then be the driver for the improvement of the production process and for the research and constructive validation of the façade panel, leveraging both the deformability of the textile support and the necessary additional preliminary fabric cutting and sewing processes.

Given the countless configurations that the proposed shading system based on the geometrical parameters in section 2.3, using a parameterization process analysis, a meaningful solution space of the geometric configurations cannot be easily defined. Therefore, to automatize and reduce the number of iterations of a solution space with thousands of possible outputs, a stochastic optimization technique that was chosen based on evolutionary algorithms such as genetic optimization algorithms.

For the genetic optimization process, Octopus (Yassin Ashour, 2015), a Grasshopper plug-in, was used. The generative performance-based design exploration included six geometrical parameters as genomes (panel height (h), panel width (w), diameter (d), shading depth (t), hole rotation (ϕ) and hole tilt (θ)) and two optimization objectives (fitness function) based on daylight metrics objectives:

- (1) sUDI, with a threshold of 75% of the analysis area between 100 and 2,000 Lux, as described in the Konis paper (Konis *et al.*, 2016).
- (2) Simplified daylight glare probability (sDGP), no greater than 0.35 for more than 100 h (Wienold, 2009).

The GA's objective is to maximize the percentage of sUDI, and at the same time, minimize the number of glare hours above 0.35. sUDI was chosen as an inclusive metric to consider daylight availability, uniformity distribution across space and potential overheating. To quantify glare potential, sDGP was selected over DGP to reduce the computational time.

Finally, the best solutions generated by the GA were compared against traditional solar shading configurations, such as meter overhang and horizontal louvres with a width-spacing ratio of 1, as a performance benchmark.

Shading systems performance is compared using the following daylighting metrics: DA, UDI between 100 and 2,000 Lux and over 2,000 Lux, glare hours across the year, and details imaged based DGP for typical days of the year based on a single viewpoint placed at 2 m away from the facade facing outside.

4. Results and discussion

4.1 Experimental results

Spectral and total reflectance values for the white samples presented in Figure 2 are shown in Figure 8. It is possible to observe the same trend in the reflectance curves, with a shift between them. Integral visible values range between 0.67 and 0.8. Samples were prepared

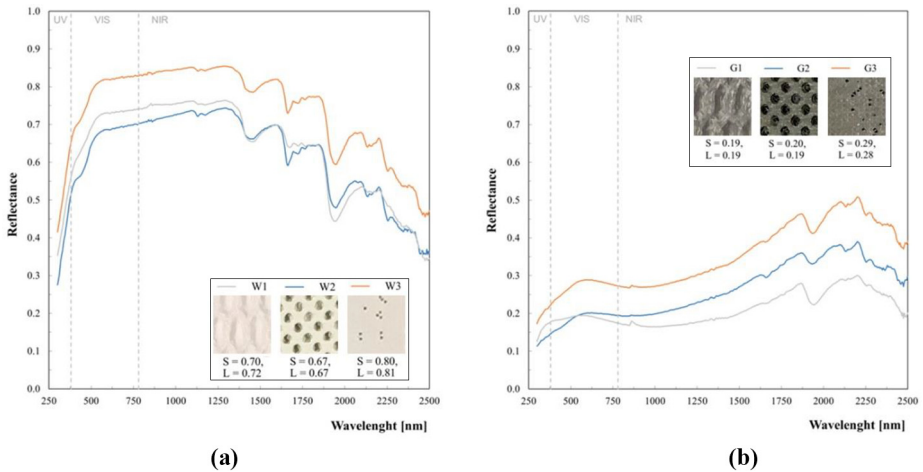


Figure 8. Spectral reflectance curve

Notes: (a) Reflectance white samples with a different texture; (b) reflectance grey samples with a different texture

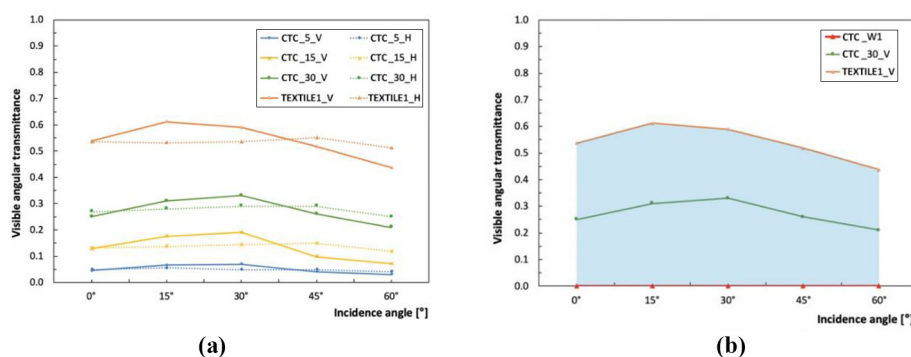
Source: Created by author

using the same cement white mix; for this reason, reflectance variations are dependent on the surface texture of the fabric. In sample W2, the presence of small cavities affects the overall reflectance value with a drop of about 15% compared to a continuous surface as W3. Whereas W1, the increased roughness due to embossed rhomboidal texture probably determines the lower spectral and total reflectance compared to the uniform sample. All the broadband and spectral data are the averages of three measurements of each sample obtained by moving the sample on the right and left of the sample port. The same optical behaviour has been discerned for the grey samples. Curves show the same trend with high reflectance values in the last part of the NIR band ($2,300\text{ }\mu\text{m}$) and a gradual decrement in the first part of the NIR and the visible spectral area. Reflectance values are included between the range of 0.19 for G1 and 0.29 for G3. The pit around $2,000\text{ nm}$ is typical of the spectral signature of the cementitious material.

In Figure 9, the visible angular transmittance values of the three translucent specimens and the 3D fabric without cement addition (Textile 1) are presented. Observing the angular transmittance behaviour in Figure 9(a), it is possible to notice that for the samples CTC_5, CTC_15 and CTC_30, the angular dependency of the CTC samples was found to be relatively insignificant, particularly in the horizontal position, and their angular behaviour tended to decrease as the samples became less translucent. It was observed that each CTC sample exhibited a cusp at an angle of incidence of 30° , which is likely due to internal reflection caused by the fabric geometry and the cement matrix within the spacer. The cusp in the CTC samples is shifted by 15° and less pronounced compared to Textile 1 (sample without cement); this means that cement tends to reduce the specular transmission and redistribute the angular transmittance behaviour improving the scattering of the sample. In Figure 9(b), the blue area defines the estimated possible transmittance range achievable by combining this type of spacer fabric and cement. As shown in Figure 9(b), the average transmission in the visible spectrum can vary from 5% for CTC_5 to 30% for CTC_30. Spectral and integral values obtained are used for the material definitions in Radiance.

4.2 Performance simulation

To select the most appropriate translucent material definition to simulate the optical behaviour of CTC, the two Trans material definitions were compared using as a benchmark the measured



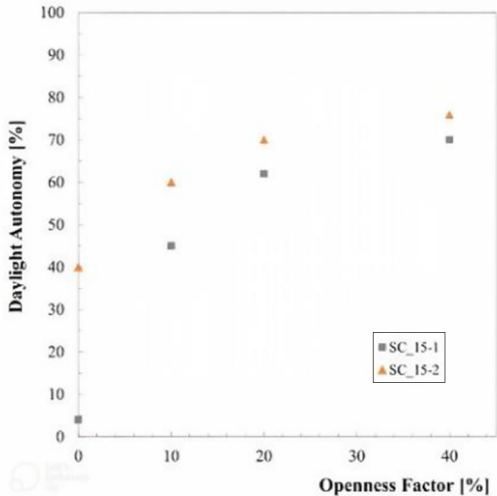
Notes: (a) Angular dependence for four different translucent samples – left; (b) area of possible transmittance value based on samples light permeability from 5% to 55% – right
Source: Created by author

Figure 9.
Visible angular
transmittance value

values. The preliminary simulation found a better accordance between planar measured samples and the model created in accordance with Reinhart and Andersen (2006). As an additional result, Figure 10 shows a significant difference between the two “Trans” Radiance material definitions, with 15% visible transmission, for a reference shading geometry and in a DA assessment. The first (SC_15-1) is based on Mead (2012) and the second (SC_15-2) refers to Reinhart and Andersen (2006). The test bed for the analysis was represented by shading screens placed outside the glazed surface; the difference in DA reaches 70%–80%. For the other configurations, the divergence becomes less significant due to the influence of direct light passing through the shading screen openings. However, it remains significant, respectively, around 25% and 15% for the 10% and 20% openness factor.

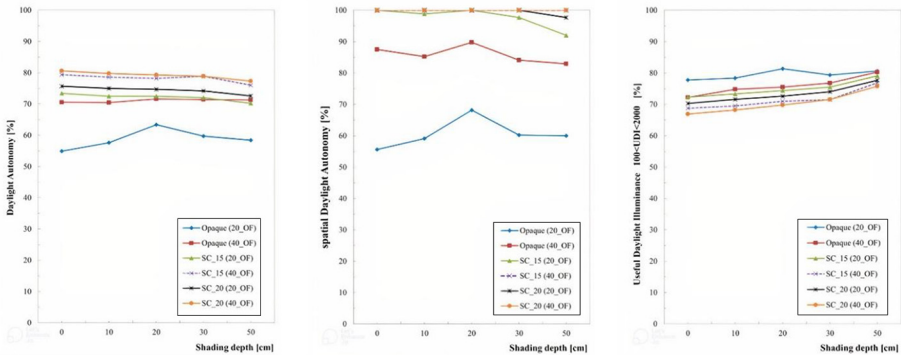
Figure 11(a) shows that, for the translucent materials (SC), DA slightly decreases when increasing the depth of the funnel (shading depth on the *x*-axis); however, DA curves do not

Figure 10.
Daylight autonomy
(DA) comparison
between different
CTC material
definitions



Source: Created by author

Figure 11.
Daylight autonomy,
spatial daylight
autonomy and useful
daylight illuminance
varying the depth of
the funnel shading



Source: Created by author

present a significant drop due to the diffuse light that passes through. On the other hand, considering an opaque configuration for the material performs worse for the overall DA percentage, making it lower than 70%. In particular, due to the funnel effect, for opaque configurations, sDA increases from 55% to 65% for funnel depth between 0 and 20 cm and then decreases for deeper solutions. This trend is also confirmed for the sDA and UDI metrics (Graphs 2 and 3), where the same peak value is visible for 20 cm funnel depth.

The translucent solutions present a more linear trend with an increment of UDI percentage (between 100 and 2,000 Lux) increasing the depth due to the reduction of overlit area. With an overall higher performance considering both UDI and DA, for shading depth around 20–30 cm.

Figure 7 shows the solutions space obtained from the GA after ten iterations and more than 700 simulations. The red dots in the graph represent the optimized solutions on the Pareto front. All the solutions marked with red dots achieve the thresholds of sUDI and sDGP defined in Section 4.2. The most effective configuration generated by the GAs can achieve a DA = 75%, sDA = 80%, $UDI_{100-2,000} = 82\%$, a $sUDI_{100-2,000} = 95\%$ and simultaneously can reduce the hours of disturbing and intolerable to 60 per year. GAs applied to the geometrical optimization of the shading system represents an effective methodology to investigate a wide solution space and identify a range of possible solutions.

4.3 Comparison with traditional shading systems

Some optimized results derived from the previous analysis are selected and compared to two standard alternative shading systems and an unshaded baseline for the reference office building exposed south. The alternatives description is listed in the first column of Figure 12. Focusing on the DA results in Figure 12 appears that traditional solutions perform better since the average values are greater, around 90% compared to 75%. However, considering the UDI between 100 and 2,000 Lux and over 2,000 Lux, it is possible to comprehend how the funnel solutions can reach a higher level of daylight performance in terms of visual comfort. The funnel-shaped geometries can more effectively limit the oriented incoming light reducing the undesired amount of daylight over 2,000 Lux, a possible source of glare and potential overheating.

The funnel shading system with regular geometry (SC_15) compared to a louvre system can reduce the amount of overlit hours from 32.4% to 14.9% and guarantee a sufficient level of illuminance for 75.3%. Adopting the fully optimized shading system through GA (SC_15_GA with variable OF, depth, openings orientation angles theta and phi) is possible to increase the UDI, between 100 and 2,000 Lux up to 82%. Even though the mean value of DA is lower for funnel configurations, observing the light spatial distribution, it is possible to see that in the first 2/3 of the room, where a reference desk can be placed, the DA value is greater than 80% (Table 1).

In the absence of an internal roller shade, Figure 13 shows the number of hours of glare for each solution. As you can see, a significant improvement was obtained in the reduction of annual glare. A fully glazed unshaded façade ($WWR = 75\%–80\%$) presents several glare hours (around 800), requiring the installation of internal roller shades with low light transmission. A traditional external static solar shading system, such as an overhang or louvres, can reduce the discomfort glare hours by up to 70%, respectively, with 500 and 250 h per year. However, considering the substantial amount of glare hours and high illuminance levels, the current solutions still require an internal roller shade. With the proposed funnel solutions is possible to decrease the disturbing and intolerable glare hours by another 60%–70%.

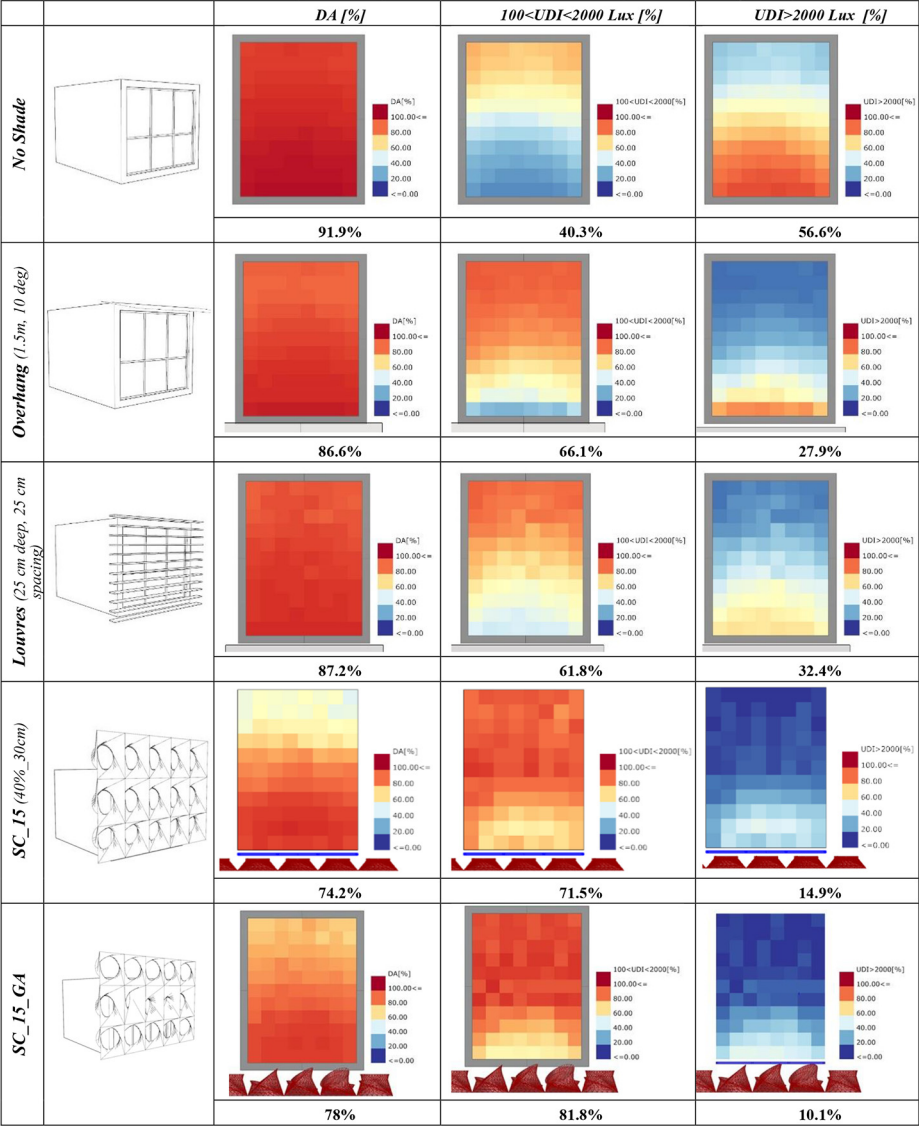


Figure 12.
Daylighting results
(DA and UDI) for
different façade
configurations

Source: Created by author

The same metrics investigated previously for the south façade were also assessed for the west façade. As shown in [Figure 13](#), a customized funnel shading system can achieve a high level of daylight performance in terms of annual illuminance and glare for the west orientation. The sDA is equal to 92%, a value following the south-facing curtain wall. Besides, the UDI in the well-light range reaches a high percentage value, around 80%–85%.

In addition, through geometry optimization and self-shading, the hours of glare are under 100 per year.

4.4. A focus on the glare-controlling capabilities

In this section, the results of hourly glare (DGP) were compared for four different façade configurations (no external shade, Louvres, SC_15_GA and SC_Variable_GA with translucency distribution based on glare risk area). Four critical days during the year were considered for the south-exposed scenario. For SC_variable_GA, the shading area hit by the highest amount of light over the annual period is characterized by low transmission values (opaque or total transmission 5%), while the other parts gradually increase the transparency to higher values ranging from 15 to 30% in transmissivity.

As shown in Figure 14, standard solutions, such as fully glazed façades and louvres, have several hours, which exceed the glare comfort limit ($DGP < 0.35$); basically, for all afternoon, the user could be disturbed by glare phenomena. The user is placed aside the window on a side-lit desk. With the proposed funnel solution, intolerable glare occurs only for an hour a day during January and February, with DGP values over 0.4 (SC_15_GA). In the latter case, the translucency of the material is kept constant along the entire surface, with the properties uniformly distributed over the surface. On the other hand, it is also possible to add a local variation of transparency as an additional variable of the optimization process, leading to an alternate between translucent surfaces and completely opaque portions of the

Case	Perceptible glare [h]	Disturbing glare [h]	Intolerable glare [h]
No shading	275	169	376
Overhang	231	70	211
Louvres 1–1	39	19	214
SC_15 (40%_30cm)	31	10	58
SC_15_GA	13	5	38

Table 1.

Annual glare results –
only working hours in
the range 8–17 or
9–18 were taken into
account

Note: The overhang is 1.5 m long, and the louvres have depth and spacing both equal to 25 cm (45° cut-off angle)

Source: Created by authors

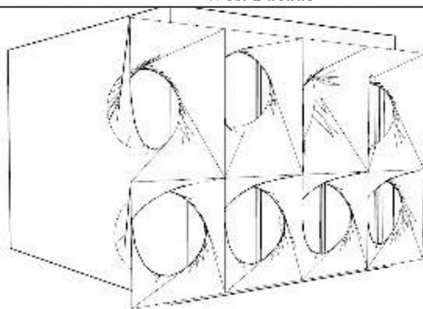
West Façade		Daylighting metrics	
		DA	71
		UDI < 100	10.5
		100 < UDI < 2000	83.8
		UDI > 2000	5.6
		sDA	92.1
		DF	2.2
		Glare [h]	
		Perceptible glare	33
		Disturbing glare	16
		Intolerable glare	40

Figure 13.

Daylighting (DA and
UDI) and annual
glare for optimized
fabric concrete
shading system.
Milan, west façade

Source: Created by author

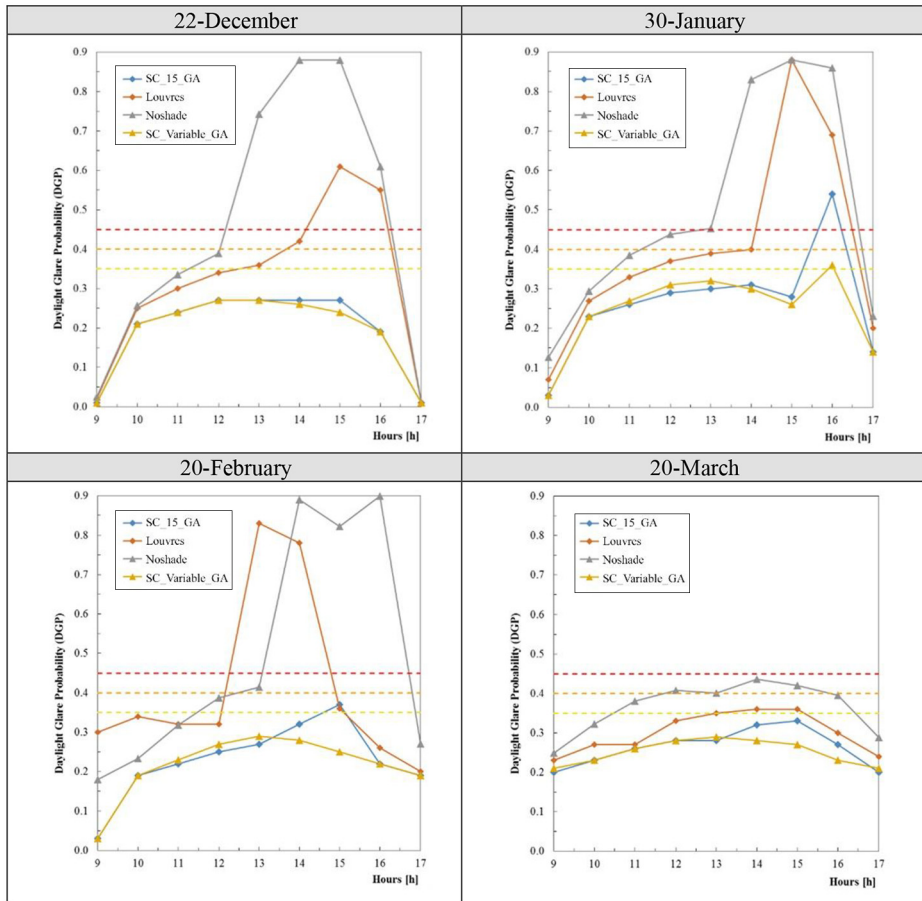


Figure 14.
Daylight glare
probability on a
point-in-time basis.
Glare viewpoint
facing west, 2 m
away from façade

Source: Created by author

shading element. In this way, glare control (SC_Variable_GA) can be made more effective. Translucency control on the funnel surfaces is shown by the yellow line in the following graphs. With this approach is then possible to decrease the glare probability under 0.35, without any internal shading system, for all the typical working hours.

5. Conclusions

The use of computational design tools and methods, specifically the Rhinoceros software and Grasshopper platform, has allowed for the development of a novel tool and process for the design of high-performance external shading systems using an innovative high-performance CTC material. The paper introduces a novel material for façade application and its implementation in an occupant-centric generative design workflow to exploit its capabilities, to develop high-performance solar shading systems. This approach involves defining the relationships between design strategies and parameters that reflect shape and performance constraints, as well as environmental performance.

The sUDI and sDGP in a multi-objective GA represent appropriate fitness functions able to generate a consistent space solution taking into account both visual comfort and daylighting performance. The case study shows that tailor-made shading systems can be considered a better alternative to traditional static shading elements like louvres or overhangs. In addition, by taking advantage of high material customization in terms of shape optimization and control of translucency, it is possible to achieve daylighting and visual comfort performance virtually unattainable with the current external static cement-based shading devices. To be cost-effective, the optimization process must be able to link project goals with the production process, morphological limits and expected performance in use.

The results showed that the proposed funnel shape coupled with the CTC material could generate a well-lit space free of disturbing glare without a consistent need of roller shades, for different orientations and in a simpler and cheaper way compared to other solutions.

Although the production process of the material is based on a parametric logic for the easy realization of complex shapes, possible deformations of the material have been estimated, which require further investigation to be verified. The proposed tool and process aim to bridge the gap between design and manufacturing, enabling the creation of tailored solutions for specific context conditions through a simple production process.

The proposed findings are considered preliminary investigations to evaluate the application of the system in construction. It was demonstrated that it is possible to efficiently rationalize design problems where geometric and environmental parameters must be optimized together through the assessment of the performance of a large number of alternative solutions according to Pareto's optimum.

The space of the solution does not include all possibilities. The realization of physical samples is required to verify the hypotheses. In fact, for the sake of simplicity, some specific geometric issues were not considered, such as local changes of geometry due to wrinkles and overlapping of fabric flaps in correspondence of internal surfaces with less curvature. In addition, and with the purpose of further development, the proposed workflow should focus on:

- Measure the angular optical properties of CTC by using a photo-goniometer to obtain a BSDF for each translucency state; and
- Implement BSDF in complex geometry shading systems to improve the accuracy of the model to be developed in a Radiance five-phase method environment.

References

- Arumi-Noe, F. (1996), "Algorithm for the geometric construction of an optimum shading device", *Automation in Construction*, Vol. 5 No. 3, pp. 211-217.
- Azadeh, O. (2011), "Design optimization of a contemporary high performance shading screen – integration of 'form' and simulation tools", *Proceedings of Building Simulation 2011: 12th Conference of International Building Performance Simulation Association*, pp. 2491-2498.
- Banthia, N., Bindiganavile, V., Jones, J. and Novak, J. (2012), "Fiber-reinforced concrete in precast concrete applications: research leads to innovative products", *PCI Journal*, Vol. 57 No. 3, pp. 33-46.
- Brembilla, E., Hopfe, C.J. and Mardaljevic, J. (2017), "Influence of input reflectance values on climate-based daylight metrics using sensitivity analysis", *Journal of Building Performance Simulation*, Vol. 11 No. 3, pp. 1-17.

-
- Caldas, L.G. and Norford, L.K. (2003a), "Genetic algorithms for optimization of building envelopes and the design and control of HVAC systems", *Journal of Solar Energy Engineering*, Vol. 125 No. 3, pp. 343-351.
- Caldas, L.G. and Norford, L.K. (2003b), "Shape generation using Pareto genetic algorithms: integrating conflicting design objectives in low-energy architecture", *International Journal of Architectural Computing*, Vol. 1 No. 4, pp. 503-515.
- Carlucci, S., Causone, F., De Rosa, F. and Pagliano, L. (2015), "A review of indices for assessing visual comfort with a view to their use in optimization processes to support building integrated design", *Renewable and Sustainable Energy Reviews*, Vol. 47, pp. 1016-1033.
- Eigensatz, M., Kilian, M., Schiftner, A., Mitra, N.J., Pottmann, H. and Pauly, M. (2010), "Paneling architectural freeform surfaces", *ACM Transactions on Graphics*, Vol. 29 No. 4.
- González, J. and Fiorito, F. (2015), "Daylight design of office buildings: optimisation of external solar shadings by using combined simulation methods", *Buildings*, Vol. 5 No. 2, pp. 560-580.
- Gosselin, C., Duballet, R., Roux, P., Gaudillière, N., Dirrenberger, J. and Morel, P. (2016), "Large-scale 3D printing of ultra-high performance concrete – a new processing route for architects and builders", *Materials and Design*, Vol. 100, pp. 102-109.
- Han, F., Chen, H., Li, X., Bao, B., Lv, T., Zhang, W. and Duan, W.H. (2016), "Improvement of mechanical properties of concrete canvas by anhydrite-modified calcium Sulfoaluminate Cement", *Journal of Composite Materials*, Vol. 50 No. 14, pp. 1937-1950.
- Hashemloo, A., Inanici, M. and Meek, C. (2016), "GlareShade: a visual comfort-based approach to occupant-centric shading systems", *Journal of Building Performance Simulation*, Vol. 9 No. 4, pp. 351-365.
- Henriksen, T. (2017), "Advancing the manufacture of complex geometry GFRC for today's building envelopes", A+BE | Architecture and the Built Environment, available at: <https://journals.open.tudelft.nl/abe/about>
- Henriksen, T., Lo, S. and Knaack, U. (2015), "An innovative approach to manufacture thin-walled glass fibre reinforced concrete for tomorrow's architectural buildings envelopes with complex geometries", *Journal of Building Engineering*, Vol. 4, pp. 189-199.
- Kabre, C. (1998), "Winshade: a computer design tool for solar control", *Building and Environment*, Vol. 34 No. 3, pp. 263-274.
- Katsifaraki, A., Bueno, B. and Kuhn, T.E. (2017), "A daylight optimized simulation-based shading controller for Venetian blinds", *Building and Environment*, Vol. 126, pp. 207-220.
- Konis, K., Gamas, A. and Kensek, K. (2016), "Passive performance and building form: an optimization framework for early-stage design support", *Solar Energy*, Vol. 125, pp. 161-179.
- Kuhn, T.E. (2017), "State of the art of advanced solar control devices for buildings", *Solar Energy*, Vol. 154, pp. 112-133.
- Li, W., Lin, X., Bao, D.W. and Min Xie, Y. (2022), "A review of formwork systems for modern concrete construction", *Structures*, Vol. 38, pp. 52-63.
- Liu, J. and Lv, C. (2022), "Properties of 3D-Printed polymer fiber-reinforced mortars: a review", *Polymers (Basel)*, Vol. 14 No. 7, p. 1315.
- Maccari, A., Montecchi, M., Treppo, F. and Zinzi, M. (1998), "CATRAM: an apparatus for the optical characterization of advanced transparent materials", *Applied Optics*, Vol. 37 No. 22, pp. 5156-5161.
- Madkour, Y. (2023), "Computational shading".
- Mainini, A.G., Poli, T., Zinzi, M. and Cangiano, S. (2012), "Spectral light transmission measure and radiance model validation of an innovative transparent concrete panel for facades", *Energy Procedia*, Vol. 30, pp. 1184-1194.

-
- Marsh, A. (2005), "The application of shading masks in building simulation", in *IBPSA 2005 International Building Performance Simulation Association 2005*, pp. 725-732.
- Mead, D. (2012), "Trans' materials – modeling and specifying a next generation".
- Omidfar, A. (2015), "Performance evaluation of complex facades using various shading systems with ornamental patterns", in *Illuminating Engineering Society (IES)*.
- Oxman, N. and Rosenberg, J.L. (2007), "Material performance based design computation: an inquiry into digital simulation of material properties as design generators", in *CAADRIA 2007 – The Association for Computer-Aided Architectural Design Research in Asia: Digitization and Globalization*, pp. 5-12.
- Poli, T., Zani, A., Speroni, A. and Mainini, A.G. (2019), "Cladding element for use in construction and method for manufacturing the same", available at: <https://patents.google.com/patent/WO2020202122A1/en>
- Rael, R. and San Fratello, V. (2011), "Developing concrete polymer building components for 3D printing", in *Integration Through Computation – Proceedings of the 31st Annual Conference of the Association for Computer Aided Design in Architecture, ACADIA 2011*, pp. 152-157, available at: <https://doi.org/10.52842/conf.acadia.2011.152>
- Rakha, T. and Nassar, K. (2011), "Genetic algorithms for ceiling form optimization in response to daylight levels", *Renewable Energy*, Vol. 36 No. 9, pp. 2348-2356.
- Reinhart, C.F. and Andersen, M. (2006), "Development and validation of a radiance model for a translucent panel", *Energy and Buildings*, Vol. 38 No. 7, pp. 890-904.
- Rörig, T., Sechelmann, S., Kycia, A. and Fleischmann, M. (2015), "Surface panelization using periodic conformal maps", *Advances in Architectural Geometry*, Vol. 2014, pp. 199-214.
- Roye, A. and Gries, T. (2007), "3-D textiles for advanced cement based matrix reinforcement", *Journal of Industrial Textiles*, Vol. 37 No. 2, pp. 163-173.
- Ruttico, P., Rossi, A., Panahikazemi, L. and Andaloro, M. (2016), "Innovative methods for mold design and fabrication", in *CIB*IAARC W119 CIC 2016 Workshop Advanced Construction and Building Technology for Society*.
- Sadeghi, S.A., Karava, P., Konstantzos, I. and Tzempelikos, A. (2016), "Occupant interactions with shading and lighting systems using different control interfaces: a pilot field study", *Building and Environment*, Vol. 97, pp. 177-195.
- Sargent, J., Niemasz, J. and Reinhart, C. (2011), "SHADERADE: combining rhinoceros and EnergyPlus for the design of static exterior shading devices", *Build Simulator*, Vol. 11, pp. 1-9.
- Sherif, A., Sabry, H. and Rakha, T. (2012), "External perforated solar screens for daylighting in residential desert buildings: identification of minimum perforation percentages", *Solar Energy*, Vol. 86 No. 6, pp. 1929-1940.
- Turrin, M., von Buelow, P. and Stouffs, R. (2011), "Design explorations of performance driven geometry in architectural design using parametric modeling and genetic algorithms", *Advanced Engineering Informatics*, Vol. 25 No. 4, pp. 656-675.
- Turrin, M., Von Buelow, P., Kilian, A. and Stouffs, R. (2012), "Performative skins for passive climatic comfort: a parametric design process", *Automation in Construction*, Vol. 22, pp. 36-50.
- Tzempelikos, A. and Chan, Y.C. (2016), "Estimating detailed optical properties of window shades from basic available data and modeling implications on daylighting and visual comfort", *Energy and Buildings*, Vol. 126, pp. 396-407.
- Tzempelikos, A. and Shen, H. (2013), "Comparative control strategies for roller shades with respect to daylighting and energy performance", *Building and Environment*, Vol. 67, pp. 179-192.
- Valeri, P., Guaita, P., Baur, R., Fernández Ruiz, M., Fernández-Ordóñez, D. and Muttoni, A. (2020), "Textile reinforced concrete for sustainable structures: future perspectives and application to a prototype pavilion", *Structural Concrete*, Vol. 21 No. 6, pp. 2251-2267.

-
- Van Den Wymelenberg, K. (2012), "Patterns of occupant interaction with window blinds: a literature review", *Energy and Buildings*, Vol. 51, pp. 165-176.
- Van Den Wymelenberg, K. and Inanici, M. (2014), "A critical investigation of common lighting design metrics for predicting human visual comfort in offices with daylight", *LEUKOS*, Vol. 10 No. 3, pp. 145-164.
- Wienold, J. (2009), "Dynamic daylight glare evaluation", in *IBPSA 2009 – International Building Performance Simulation Association 2009*, pp. 944-951.
- Yassin Ashour, B.K. (2015), "Optimizing creatively in multi-objective optimization", *SIMAUD*, pp. 59-66.
- Zani, A., Andaloro, M., Deblasio, L., Ruttico, P. and Mainini, A.G. (2017), "Computational design and parametric optimization approach with genetic algorithms of an innovative concrete shading device system", *Procedia Engineering*, Vol. 180, pp. 1473-1483.

Corresponding author

Alberto Speroni can be contacted at: alberto.speroni@polimi.it